Increased Productivity of an Automated Tape Winding Process: SPIDE-TP Platform

Divya SHAH

Supervisors: B. Courtemanche; S. Caro; A. Pashkevich

Master Thesis Defense

29 August, 2017

- Extensive use in recent times
- Excellent material properties

Mike Garry. *Polymer Composites vs. Steel.*

- Extensive use in recent times
- Excellent material properties
- Manufacturing of high performance structures
- Applications: Aerospace & Automotive Industries

Mike Garry. *Polymer Composites vs. Steel.*

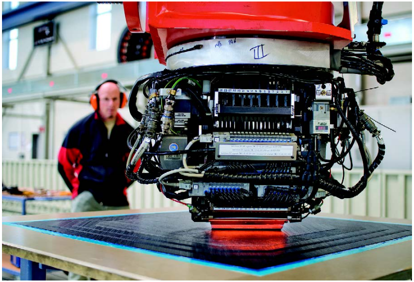

- **Automated Tape Laying (ATL)**
- Laying on molds
- Shape limitations

George Marsh (2011). "Automating aerospace composites production with fibre placement". In: *REINFORCED plastics*

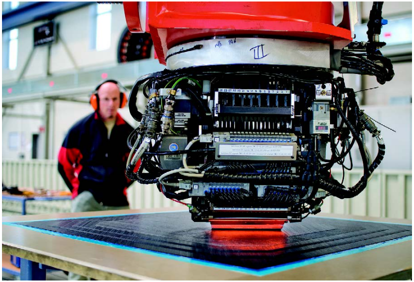

- **Automated Tape Laying (ATL)**
- Laying on molds
- Shape limitations

- **Automated Tape Winding (ATW)**
- Workpiece on rotating mandrel
- Complex geometries

George Marsh (2011). "Automating aerospace composites production with fibre placement". In: *REINFORCED plastics*

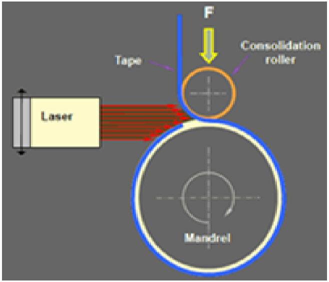

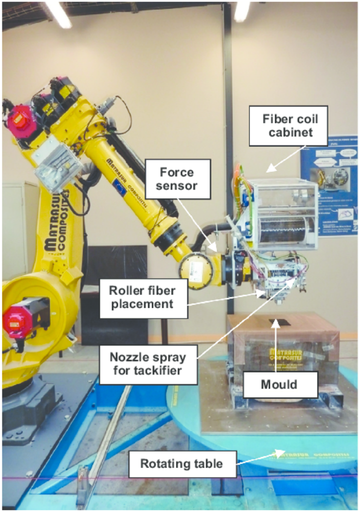

Mariem Belhaj et al. (2013). "Dry fiber automated placement of carbon fibrous preforms". In: *Composites Part B: Engineering*

Advantages

- Precise control of placement head
- In-situ consolidation
- Repeatability

Advantages

- Precise control of placement head
- In-situ consolidation
- Repeatability

Challenges

- Kinematic redundancy management
- Manipulator motion planning

Advantages

- Precise control of placement head
- In-situ consolidation
- Repeatability

Challenges

- Kinematic redundancy management
- Manipulator motion planning

Solution

- Graph-based Discrete Optimization

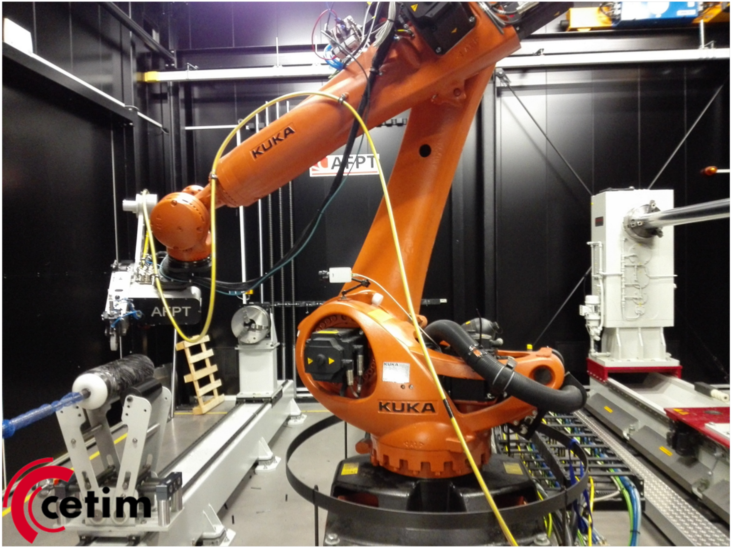

Centre technique des industries mécaniques [CETIM].

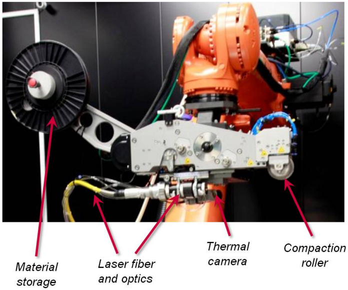

- **Different Winding Axes**
- Large Axis: Diameter 0.25m to 2.50m
- Small Axis: Diameter 25mm to 500mm

- **Winding Head Assembly**
- Laser (4kW)
- Thermal Camera
- Compaction Roller

Centre technique des industries mécaniques [CETIM].

Current Methodology

- Composicad software: Workpiece modelling & Track generation

- Post-processor: Robot program

Centre technique des industries mécaniques [CETIM].

Current Methodology

- Composicad software: Workpiece modelling & Track generation
- Post-processor: Robot program

Key Challenges

- Kinematic redundancy not fully exploited
- Discontinuities in the trajectory
- High Raw material cost

Centre technique des industries mécaniques [CETIM].

- Estimate maximum production time of a given track
- Identify the limiting axis
- Select the tools to manage kinematic redundancy
- Estimate the gain of productivity expected
- Implement proposed methods

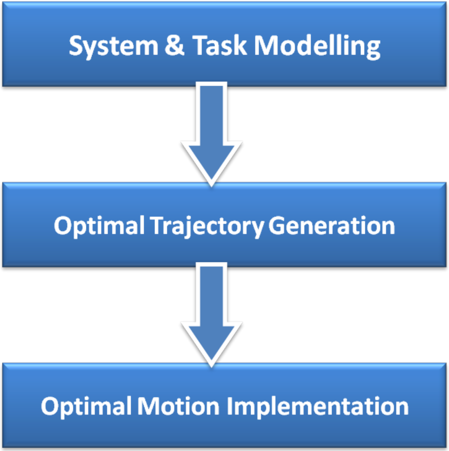
System & Task Modelling
Optimal Trajectory Generation
Optimal Motion Implementation

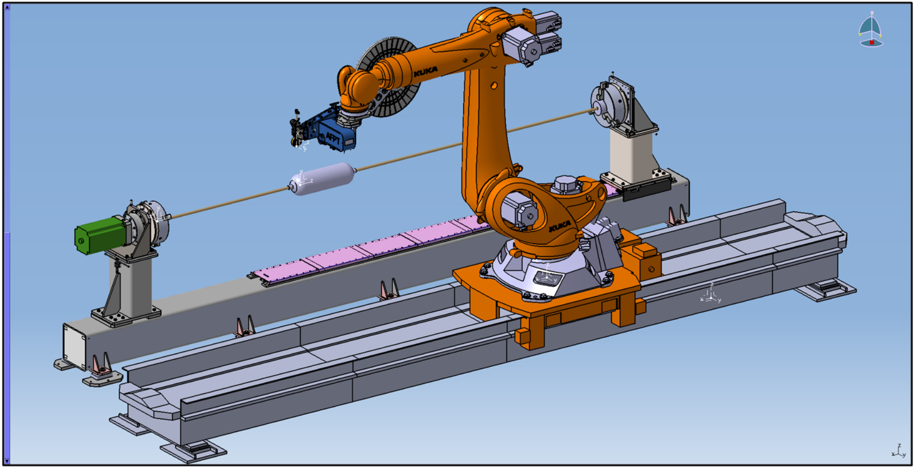
KUKA
KUKA
AFPT

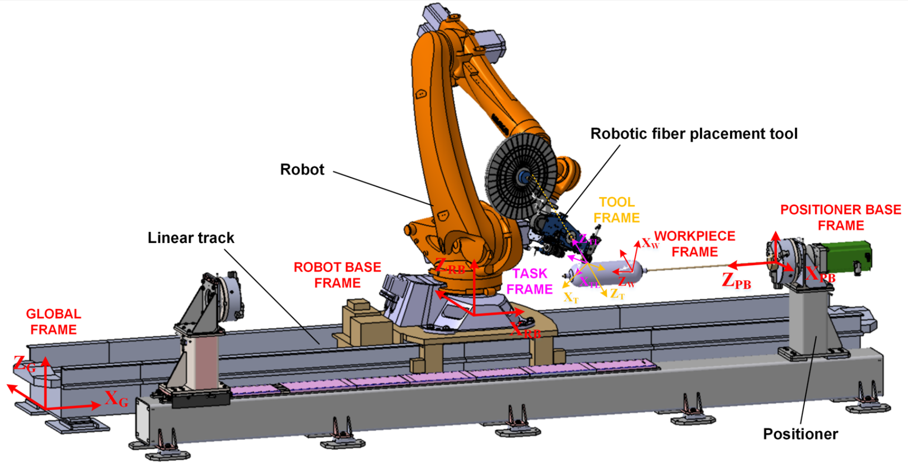
Robotic fiber placement tool
Robot
TOOL FRAME
POSITIONER BASE FRAME
Linear track
WORKPIECE FRAME
ROBOT BASE FRAME
TASK FRAME
GLOBAL FRAME
Positioner

Robot Model

$$rob(\vec{q_r}) = {}^{RB}T_1(q_1).{}^{1}T_2(q_2).{}^{2}T_3(q_3).{}^{3}T_4(q_4).{}^{4}T_5(q_5).{}^{5}T_{RF}(q_6) \quad (1)$$

Winding Axis Model

$$pos(q_p) = Rot_Z(q_p) \quad (2)$$

Linear Axis Model

$$lin(q_l) = Trans_X(q_l) \quad (3)$$

Robot Model

$$\boldsymbol{rob}(\vec{\boldsymbol{q}}_{\boldsymbol{r}}) = {}^{\boldsymbol{RB}}\boldsymbol{T}_{\boldsymbol{1}}(q_1).{}^{\boldsymbol{1}}\boldsymbol{T}_{\boldsymbol{2}}(q_2).{}^{\boldsymbol{2}}\boldsymbol{T}_{\boldsymbol{3}}(q_3).{}^{\boldsymbol{3}}\boldsymbol{T}_{\boldsymbol{4}}(q_4).{}^{\boldsymbol{4}}\boldsymbol{T}_{\boldsymbol{5}}(q_5).{}^{\boldsymbol{5}}\boldsymbol{T}_{\boldsymbol{RF}}(q_6) \quad (1)$$

Winding Axis Model

$$\boldsymbol{pos}(q_p) = \boldsymbol{Rot}_{\boldsymbol{Z}}(q_p) \quad (2)$$

Linear Axis Model

$$\boldsymbol{lin}(q_l) = \boldsymbol{Trans}_{\boldsymbol{X}}(q_l) \quad (3)$$

Robot Model

$$\boldsymbol{rob}(\vec{\boldsymbol{q}}_{\boldsymbol{r}}) = {}^{RB}\boldsymbol{T}_{\boldsymbol{1}}(q_1).{}^{1}\boldsymbol{T}_{\boldsymbol{2}}(q_2).{}^{2}\boldsymbol{T}_{\boldsymbol{3}}(q_3).{}^{3}\boldsymbol{T}_{\boldsymbol{4}}(q_4).{}^{4}\boldsymbol{T}_{\boldsymbol{5}}(q_5).{}^{5}\boldsymbol{T}_{\boldsymbol{RF}}(q_6) \quad (1)$$

Winding Axis Model

$$\boldsymbol{pos}(q_p) = \boldsymbol{Rot}_{\boldsymbol{Z}}(q_p) \quad (2)$$

Linear Axis Model

$$\boldsymbol{lin}(q_l) = \boldsymbol{Trans}_{\boldsymbol{X}}(q_l) \quad (3)$$

Robot Model

$$\boldsymbol{rob}(\vec{\boldsymbol{q}}_{\boldsymbol{r}}) = {}^{\boldsymbol{RB}}\boldsymbol{T}_{\boldsymbol{1}}(q_1).{}^{\boldsymbol{1}}\boldsymbol{T}_{\boldsymbol{2}}(q_2).{}^{\boldsymbol{2}}\boldsymbol{T}_{\boldsymbol{3}}(q_3).{}^{\boldsymbol{3}}\boldsymbol{T}_{\boldsymbol{4}}(q_4).{}^{\boldsymbol{4}}\boldsymbol{T}_{\boldsymbol{5}}(q_5).{}^{\boldsymbol{5}}\boldsymbol{T}_{\boldsymbol{RF}}(q_6) \quad (1)$$

Winding Axis Model

$$\boldsymbol{pos}(q_p) = \boldsymbol{Rot}_{\boldsymbol{Z}}(q_p) \quad (2)$$

Linear Axis Model

$$\boldsymbol{lin}(q_l) = \boldsymbol{Trans}_{\boldsymbol{X}}(q_l) \quad (3)$$

- Cylindrical workpiece with hemi-spherical domes on the ends.
- Winding path generated from the Composicad software.
- Current Travelling time: 14*sec*.

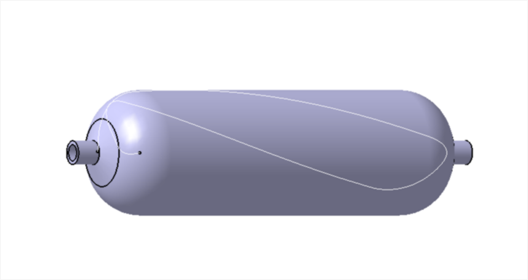

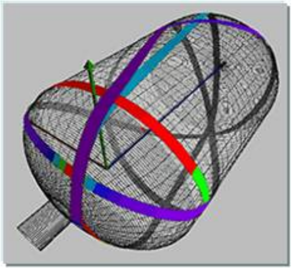

Centre technique des industries mécaniques [CETIM].

Video for the test track.

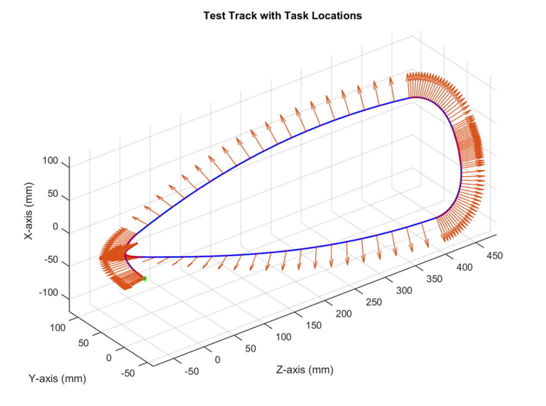

Task Model

$$ {}^{W}T_{TL_i} = \begin{bmatrix} \vec{n}_i & \vec{s}_i & \vec{a}_i & \vec{p}_i \\ 0 & 0 & 0 & 1 \end{bmatrix} = \begin{bmatrix} Rot(\vec{\varphi_i}) & \vec{p}_i \\ 0\ 0\ 0 & 1 \end{bmatrix} \Big| i = 1, 2, ..., n \qquad (4) $$

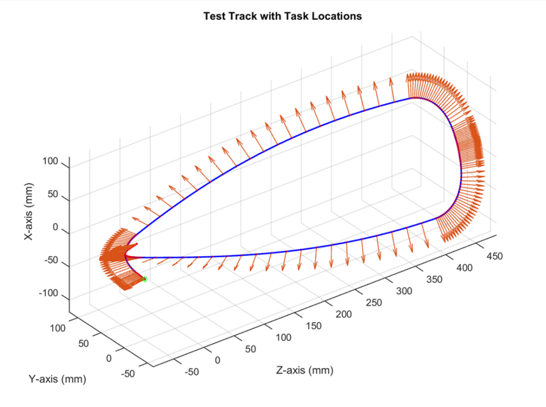

Task Model

$$^W T_{TL_i} = \begin{bmatrix} \vec{n}_i & \vec{s}_i & \vec{a}_i & \vec{p}_i \\ 0 & 0 & 0 & 1 \end{bmatrix} = \begin{bmatrix} Rot(\vec{\varphi_i}) & \vec{p}_i \\ 0\ 0\ 0 & 1 \end{bmatrix} \Big| i = 1, 2, ..., n \quad (4)$$

Task Representation

$$ {}^{0}T_{TL_i}(\vec{q_r}) = {}^{0}T_{RB}.rob(\vec{q_r}).{}^{RF}T_T.{}^{T}T_{TL_i} \quad (5) $$

$$ {}^{0}T_{TL_i}(q_p) = {}^{0}T_{PB}.pos(q_p).{}^{PF}T_W.{}^{W}T_{TL_i} \quad (6) $$

Task Constraint

$$ {}^{0}T_{RB}.rob(\vec{q_r}).{}^{RF}T_T.{}^{T}T_{TL_i} = {}^{0}T_{PB}.pos(q_p).{}^{PF}T_W.{}^{W}T_{TL_i} \quad (7) $$

Task Representation

$$^{0}T_{TL_i}(\vec{q}_r) = ^{0}T_{RB}.rob(\vec{q}_r).^{RF}T_T.^{T}T_{TL_i} \quad (5)$$

$$^{0}T_{TL_i}(q_p) = ^{0}T_{PB}.pos(q_p).^{PF}T_W.^{W}T_{TL_i} \quad (6)$$

Task Constraint

$$^{0}T_{RB}.rob(\vec{q}_r).^{RF}T_T.^{T}T_{TL_i} = ^{0}T_{PB}.pos(q_p).^{PF}T_W.^{W}T_{TL_i} \quad (7)$$

Task Representation

$$ {}^{0}\boldsymbol{T}_{\boldsymbol{TL_i}}(\vec{\boldsymbol{q}}_{\boldsymbol{r}}) = {}^{0}\boldsymbol{T}_{\boldsymbol{RB}}.\boldsymbol{rob}(\vec{\boldsymbol{q}}_{\boldsymbol{r}}).{}^{\boldsymbol{RF}}\boldsymbol{T}_{\boldsymbol{T}}.{}^{\boldsymbol{T}}\boldsymbol{T}_{\boldsymbol{TL_i}} \tag{5} $$

$$ {}^{0}\boldsymbol{T}_{\boldsymbol{TL_i}}(q_p) = {}^{0}\boldsymbol{T}_{\boldsymbol{PB}}.\boldsymbol{pos}(q_p).{}^{\boldsymbol{PF}}\boldsymbol{T}_{\boldsymbol{W}}.{}^{\boldsymbol{W}}\boldsymbol{T}_{\boldsymbol{TL_i}} \tag{6} $$

Task Constraint

$$ {}^{0}\boldsymbol{T}_{\boldsymbol{RB}}.\boldsymbol{rob}(\vec{\boldsymbol{q}}_{\boldsymbol{r}}).{}^{\boldsymbol{RF}}\boldsymbol{T}_{\boldsymbol{T}}.{}^{\boldsymbol{T}}\boldsymbol{T}_{\boldsymbol{TL_i}} = {}^{0}\boldsymbol{T}_{\boldsymbol{PB}}.\boldsymbol{pos}(q_p).{}^{\boldsymbol{PF}}\boldsymbol{T}_{\boldsymbol{W}}.{}^{\boldsymbol{W}}\boldsymbol{T}_{\boldsymbol{TL_i}} \tag{7} $$

Discretization

$$q_p^{(k)} \in [q_p^{min}, q_p^{max}]; \text{with step } \Delta q_p \tag{8}$$

Kinematic Equation

$$\boldsymbol{q_r^k}(t_i) = \boldsymbol{rob}^{-1}(\boldsymbol{pos}(q_p^{(k)}(t_i)), \mu);\ k = 0, 1...m;\ i = 1, 2..., n \tag{9}$$

Location Cell

$$\boldsymbol{L_c^{(k,i)}} = (\boldsymbol{q_r^{(k)}}(t_i), q_p^{(k)}(t_i)) \tag{10}$$

Discretization

$$q_p^{(k)} \in [q_p^{min}, q_p^{max}]; \text{with step } \Delta q_p \tag{8}$$

Kinematic Equation

$$\boldsymbol{q_r^k}(t_i) = \boldsymbol{rob}^{-1}(\boldsymbol{pos}(q_p^{(k)}(t_i)), \mu); \; k = 0, 1...m; \; i = 1, 2..., n \tag{9}$$

Location Cell

$$\boldsymbol{L_c^{(k,i)}} = (\boldsymbol{q_r^{(k)}}(t_i), q_p^{(k)}(t_i)) \tag{10}$$

Discretization

$$q_p^{(k)} \in [q_p^{min}, q_p^{max}]; \text{with step } \Delta q_p \quad (8)$$

Kinematic Equation

$$\boldsymbol{q_r^k}(t_i) = \boldsymbol{rob}^{-1}(\boldsymbol{pos}(q_p^{(k)}(t_i)), \mu); \; k = 0, 1...m; \; i = 1, 2..., n \quad (9)$$

Location Cell

$$\boldsymbol{L_c^{(k,i)}} = (\boldsymbol{q_r^{(k)}}(t_i), q_p^{(k)}(t_i)) \quad (10)$$

Discretization

$$q_p^{(k)} \in [q_p^{min}, q_p^{max}]; \text{with step } \Delta q_p \tag{8}$$

Kinematic Equation

$$\boldsymbol{q_r^k}(t_i) = \boldsymbol{rob}^{-1}(\boldsymbol{pos}(q_p^{(k)}(t_i)), \mu);\ \ k = 0, 1...m;\ \ i = 1, 2..., n \tag{9}$$

Location Cell

$$\boldsymbol{L_c^{(k,i)}} = (\boldsymbol{q_r^{(k)}}(t_i), q_p^{(k)}(t_i)) \tag{10}$$

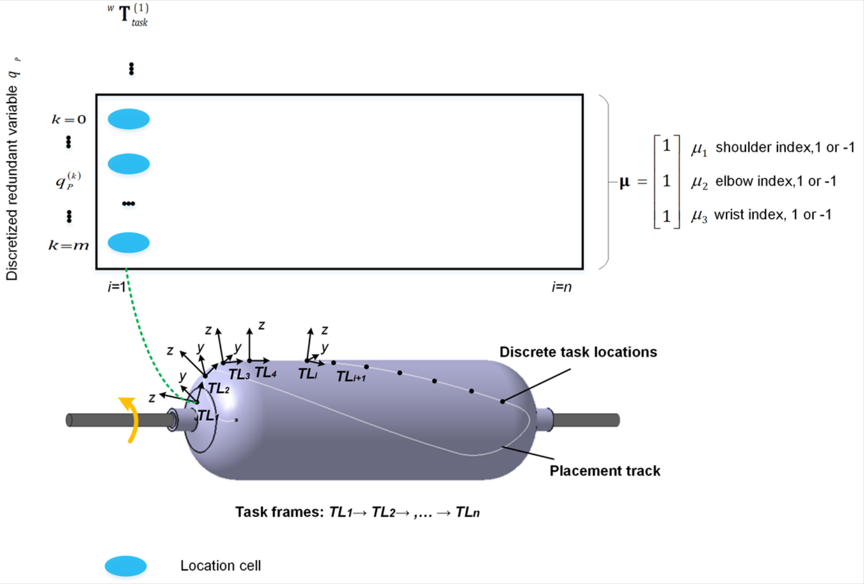

${}^{w}\mathbf{T}_{task}^{(1)}$
Discretized redundant variable q_P
$k=0$
$q_P^{(k)}$
$k=m$
$i=1$
$i=n$
$\boldsymbol{\mu} = \begin{bmatrix} 1 \\ 1 \\ 1 \end{bmatrix}$
μ_1 shoulder index,1 or -1
μ_2 elbow index,1 or -1
μ_3 wrist index, 1 or -1
Discrete task locations
Placement track
TL_1 TL_2 TL_3 TL_4 TL_i TL_{i+1}
Task frames: $TL_1 \rightarrow TL_2 \rightarrow ,\ldots \rightarrow TL_n$
Location cell

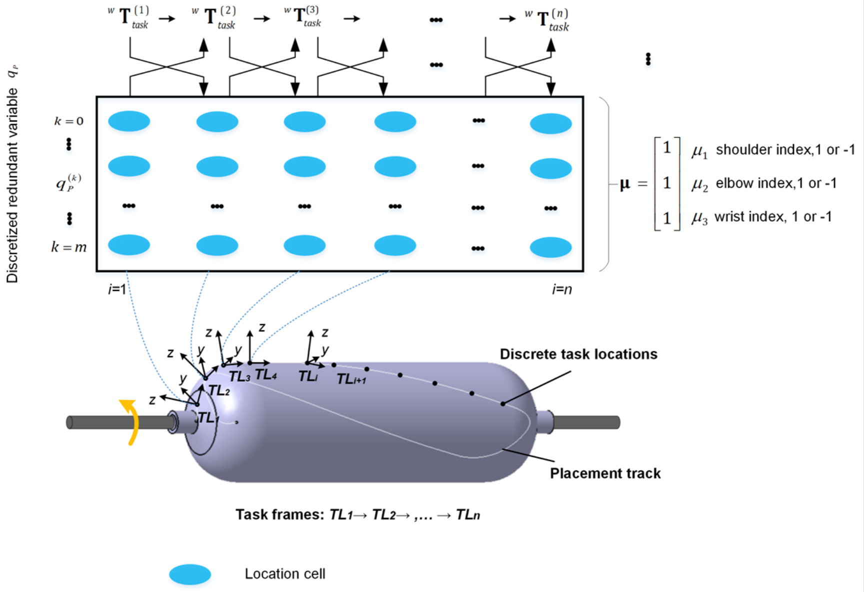

$^{w}\mathbf{T}^{(1)}_{task}$ → $^{w}\mathbf{T}^{(2)}_{task}$ → $^{w}\mathbf{T}^{(3)}_{task}$ → ... → $^{w}\mathbf{T}^{(n)}_{task}$
Discretized redundant variable q_P
$k=0$
$q_P^{(k)}$
$k=m$
i=1
i=n
$\boldsymbol{\mu} = \begin{bmatrix} 1 \\ 1 \\ 1 \end{bmatrix}$
μ_1 shoulder index,1 or -1
μ_2 elbow index,1 or -1
μ_3 wrist index, 1 or -1
Discrete task locations
TL_1 TL_2 TL_3 TL_4 TL_i TL_{i+1}
Placement track
Task frames: $TL_1 \rightarrow TL_2 \rightarrow ,\ldots \rightarrow TL_n$
Location cell

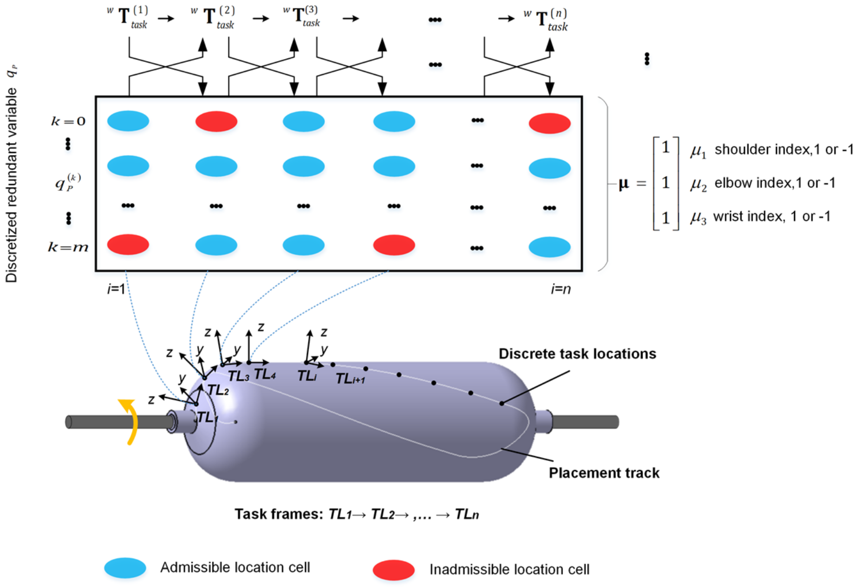
Discretized redundant variable q_P
$^{w}\mathbf{T}^{(1)}_{task}$ → $^{w}\mathbf{T}^{(2)}_{task}$ → $^{w}\mathbf{T}^{(3)}_{task}$ → ... → $^{w}\mathbf{T}^{(n)}_{task}$
$k=0$
$q_P^{(k)}$
$k=m$
i=1
i=n
$\boldsymbol{\mu} = \begin{bmatrix} 1 \\ 1 \\ 1 \end{bmatrix}$
μ_1 shoulder index,1 or -1
μ_2 elbow index,1 or -1
μ_3 wrist index, 1 or -1
Discrete task locations
Placement track
TL1 TL2 TL3 TL4 TLi TLi+1
Task frames: TL1→ TL2→ ,… → TLn
Admissible location cell
Inadmissible location cell

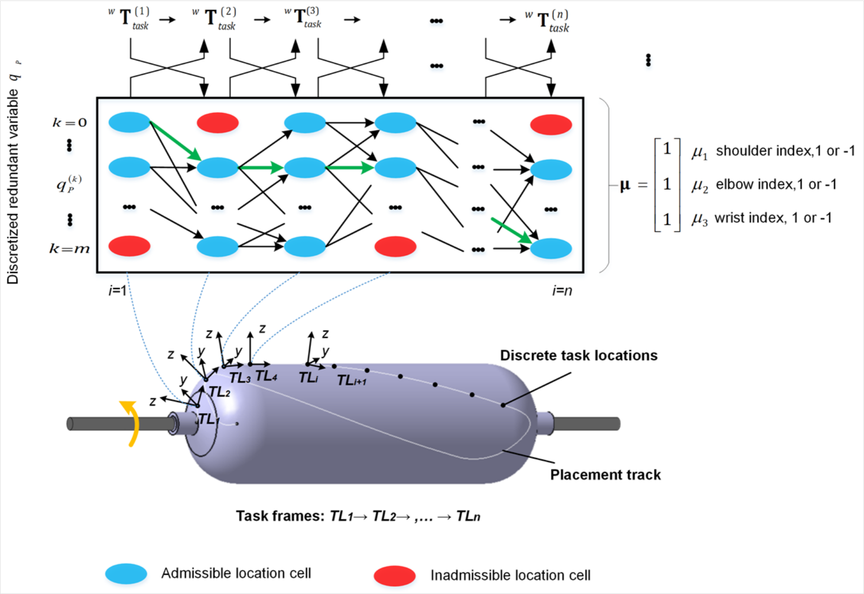
Discretized redundant variable q_P
k=0
q_P^(k)
k=m
i=1
i=n
wT_task^(1)
wT_task^(2)
wT_task^(3)
wT_task^(n)
μ = [1 1 1]
μ1 shoulder index,1 or -1
μ2 elbow index,1 or -1
μ3 wrist index, 1 or -1
Discrete task locations
Placement track
TL1
TL2
TL3
TL4
TLi
TLi+1
Task frames: TL1→ TL2→ ,... → TLn
Admissible location cell
Inadmissible location cell

Kinematic Constraints

$$\begin{aligned} q_j^{min} \leq &\quad q_j(t_i) \leq \quad q_j^{max} \\ \dot{q}_j^{min} \leq &\quad \dot{q}_j(t_i) \leq \quad \dot{q}_j^{max} \\ \ddot{q}_j^{min} \leq &\quad \ddot{q}_j(t_i) \leq \quad \ddot{q}_j^{max} \end{aligned} \tag{11}$$

where $j = 0, 1, ..., 6$ is the common index for joint variables with $j = 0$ being q_p.

Collision Constraint

$$\textbf{cols}(q_p(t), \mathbf{q_r}(t)) = 0; \; \forall \; t \in [0, T] \tag{12}$$

Kinematic Constraints

$$\begin{aligned} q_j^{min} \leq & \quad q_j(t_i) \leq \quad q_j^{max} \\ \dot{q}_j^{min} \leq & \quad \dot{q}_j(t_i) \leq \quad \dot{q}_j^{max} \\ \ddot{q}_j^{min} \leq & \quad \ddot{q}_j(t_i) \leq \quad \ddot{q}_j^{max} \end{aligned} \tag{11}$$

where $j = 0, 1, ..., 6$ is the common index for joint variables with $j = 0$ being q_p.

Collision Constraint

$$\boldsymbol{cols}(q_p(t), \boldsymbol{q_r}(t)) = 0; \; \forall \; t \in [0, T] \tag{12}$$

Video for collision detection.

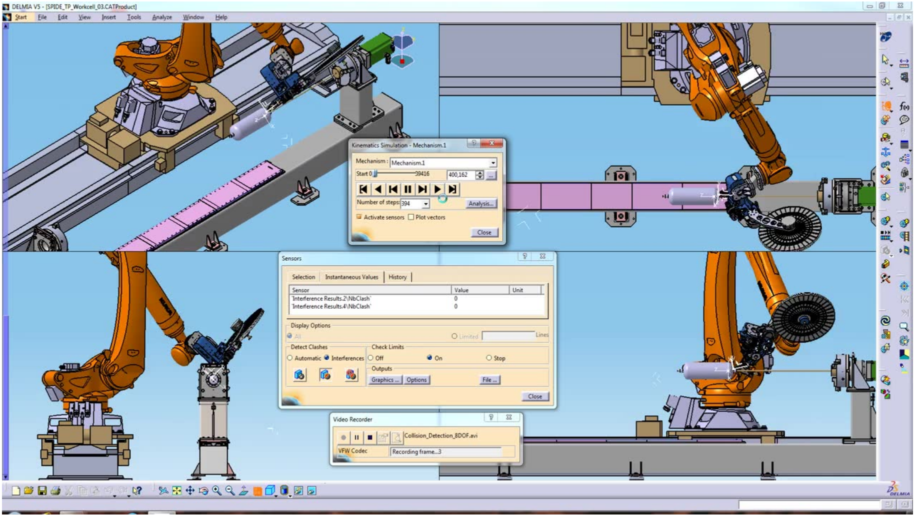

Video for testing the tool trajectory.

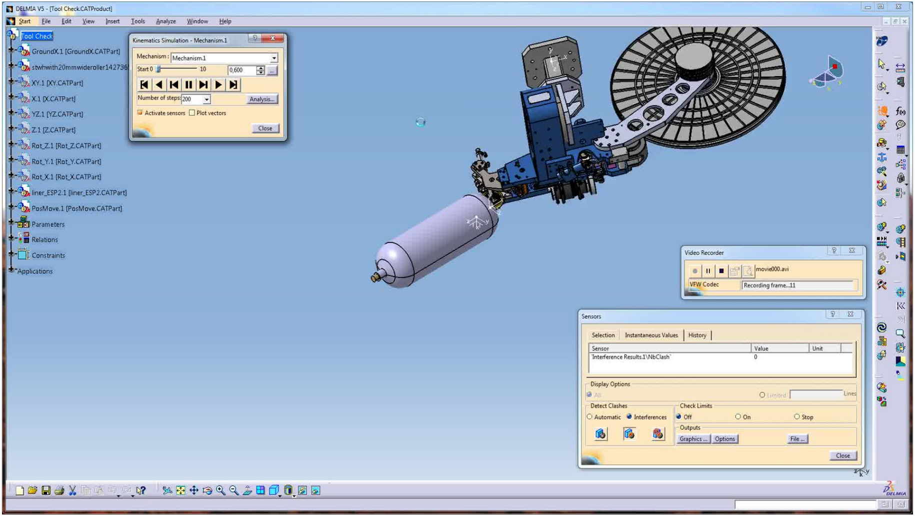

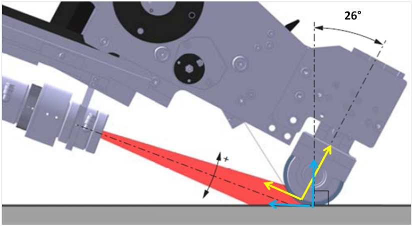

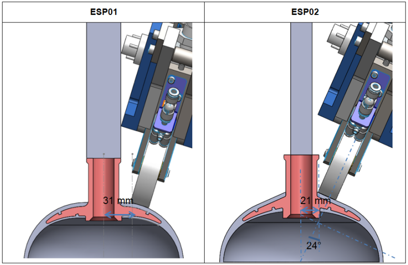

- Tool orientation correction.
- Modification of shaft geometry.

Centre technique des industries mécaniques [CETIM].

Internodal Distance

$$dist(\boldsymbol{L_c^{(k_i,i)}}, \boldsymbol{L_c^{(k_{i+1},i+1)}}) = \max_{j=0,..,6}\left(\frac{|q_{j,i}^{(k_i)} - q_{j,i+1}^{(k_{i+1})}|}{\dot{q}_j^{max}}\right) \quad (13)$$

Objective function

$$T = \sum_{j=1}^{n-1} dist(\boldsymbol{L_c^{(k_i,i)}}, \boldsymbol{L_c^{(k_{i+1},i+1)}}) \quad (14)$$

Dynamic Programming Principle

$$d_{k,i+1} = \min_{k'}\{d_{k',i} + dist(\boldsymbol{L_c^{(k,i+1)}}, \boldsymbol{L_c^{(k',i)}})\} \quad (15)$$

Jiuchun Gao, Anatol Pashkevich, and Stéphane Caro (2017). "Optimization of the robot and positioner motion in a redundant fiber placement workcell". In: *Mechanism and Machine Theory*

Internodal Distance

$$dist(\boldsymbol{L_c^{(k_i,i)}}, \boldsymbol{L_c^{(k_{i+1},i+1)}}) = \max_{j=0,..,6}\left(\frac{|q_{j,i}^{(k_i)} - q_{j,i+1}^{(k_{i+1})}|}{\dot{q}_j^{max}}\right) \tag{13}$$

Objective function

$$T = \sum_{j=1}^{n-1} dist(\boldsymbol{L_c^{(k_i,i)}}, \boldsymbol{L_c^{(k_{i+1},i+1)}}) \tag{14}$$

Dynamic Programming Principle

$$d_{k,i+1} = \min_{k'}\{d_{k',i} + dist(\boldsymbol{L_c^{(k,i+1)}}, \boldsymbol{L_c^{(k',i)}})\} \tag{15}$$

Jiuchun Gao, Anatol Pashkevich, and Stéphane Caro (2017). "Optimization of the robot and positioner motion in a redundant fiber placement workcell". In: *Mechanism and Machine Theory*

Internodal Distance

$$dist(\boldsymbol{L_c^{(k_i,i)}}, \boldsymbol{L_c^{(k_{i+1},i+1)}}) = \max_{j=0,..,6}\left(\frac{|q_{j,i}^{(k_i)} - q_{j,i+1}^{(k_{i+1})}|}{\dot{q}_j^{max}}\right) \tag{13}$$

Objective function

$$T = \sum_{j=1}^{n-1} dist(\boldsymbol{L_c^{(k_i,i)}}, \boldsymbol{L_c^{(k_{i+1},i+1)}}) \tag{14}$$

Dynamic Programming Principle

$$d_{k,i+1} = \min_{k'}\{d_{k',i} + dist(\boldsymbol{L_c^{(k,i+1)}}, \boldsymbol{L_c^{(k',i)}})\} \tag{15}$$

Jiuchun Gao, Anatol Pashkevich, and Stéphane Caro (2017). "Optimization of the robot and positioner motion in a redundant fiber placement workcell". In: *Mechanism and Machine Theory*

Internodal Distance

$$dist(\boldsymbol{L_c^{(k_i,i)}}, \boldsymbol{L_c^{(k_{i+1},i+1)}}) = \max_{j=0,..,6}\left(\frac{|q_{j,i}^{(k_i)} - q_{j,i+1}^{(k_{i+1})}|}{\dot{q}_j^{max}}\right) \tag{13}$$

Objective function

$$T = \sum_{j=1}^{n-1} dist(\boldsymbol{L_c^{(k_i,i)}}, \boldsymbol{L_c^{(k_{i+1},i+1)}}) \tag{14}$$

Dynamic Programming Principle

$$d_{k,i+1} = \min_{k'}\{d_{k',i} + dist(\boldsymbol{L_c^{(k,i+1)}}, \boldsymbol{L_c^{(k',i)}})\} \tag{15}$$

Jiuchun Gao, Anatol Pashkevich, and Stéphane Caro (2017). "Optimization of the robot and positioner motion in a redundant fiber placement workcell". In: *Mechanism and Machine Theory*

Algorithm 1: Path Planning (Dynamic Programming)

```
Data: Matrix of locations L(k,i) of size m × n
Result: Minimum path length D_min & Optimal path indices k^0(i), i = 1,2,..,n
D(k,1)=0 ;
P(k,1)=null, ∀k = 1,2,...,m ;
for i = 2 to n do
    for k = 1 to m do
        for j = 1 to m do
            if cols(L(j,i−1)) = 0 & cols(L(k,i)) = 0) & (accl(L(j,i−1), L(k,i)) = 0)
            then
                r(j) = D(j,i−1) + dist(L(k,i), L(j,i−1)) ;
            else
                r(j) = inf ;
            end
        end
        D(j,i) = min(r) ;
        P(j,i) = arg min(r) ;
    end
    D_min = min(D(k,n)) ;
    k^0(n) = arg min(r) ;
end
for i = n to 2 do
    k^0(i−1) = P(k^0(i),i) ;
end
```

Jiuchun Gao, Anatol Pashkevich, and Stéphane Caro (2017). "Optimization of the robot and positioner motion in a redundant fiber placement workcell". In: *Mechanism and Machine Theory*

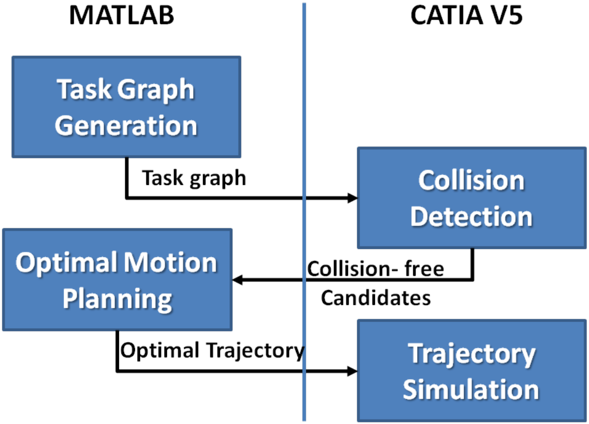
MATLAB
CATIA V5
Task Graph Generation
Task graph
Collision Detection
Optimal Motion Planning
Collision- free Candidates
Optimal Trajectory
Trajectory Simulation

Selection of the robot base location on the linear axis.

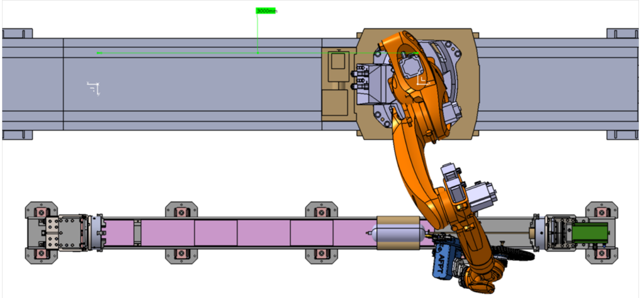

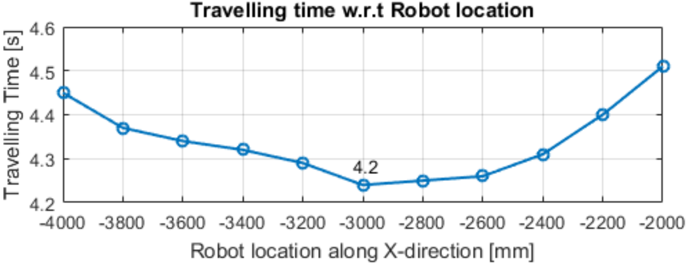

For linear axis coordinate value of $-3000mm$ and with a $1deg$ discretization step for the positioner coordinate, the results obtained are as follows:

No. of Task Locations	Travelling Time
127	$3.0sec$
200	$3.2sec$

For linear axis coordinate value of $-3000mm$ and with a $1deg$ discretization step for the positioner coordinate, the results obtained are as follows:

No. of Task Locations	Travelling Time
127	$3.0sec$
200	$3.2sec$

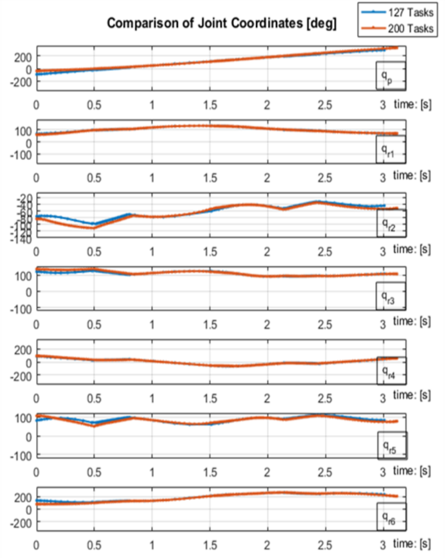

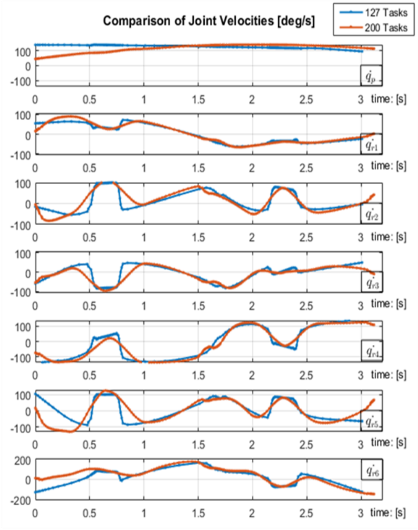
Comparison of Joint Velocities [deg/s]
127 Tasks
200 Tasks
time: [s]

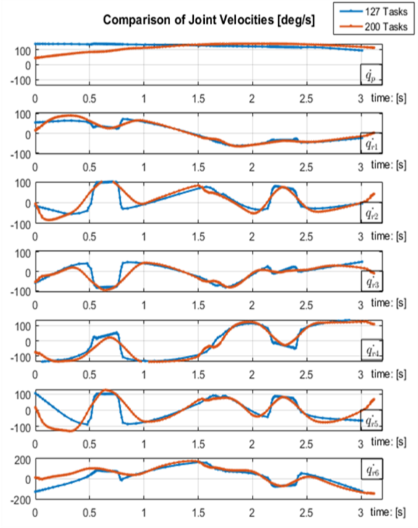
Comparison of Joint Velocities [deg/s]
127 Tasks
200 Tasks
time: [s]

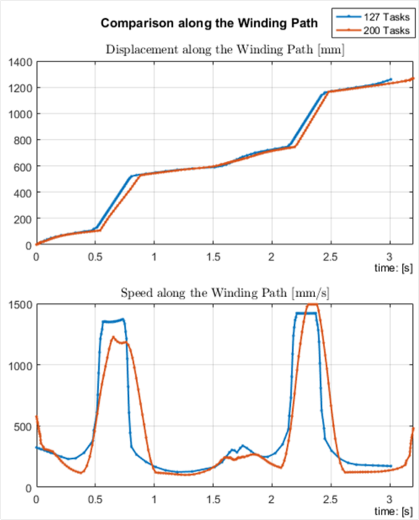
Comparison along the Winding Path
127 Tasks
200 Tasks
Displacement along the Winding Path [mm]
Speed along the Winding Path [mm/s]
time: [s]

Trajectory with 127 task locations:

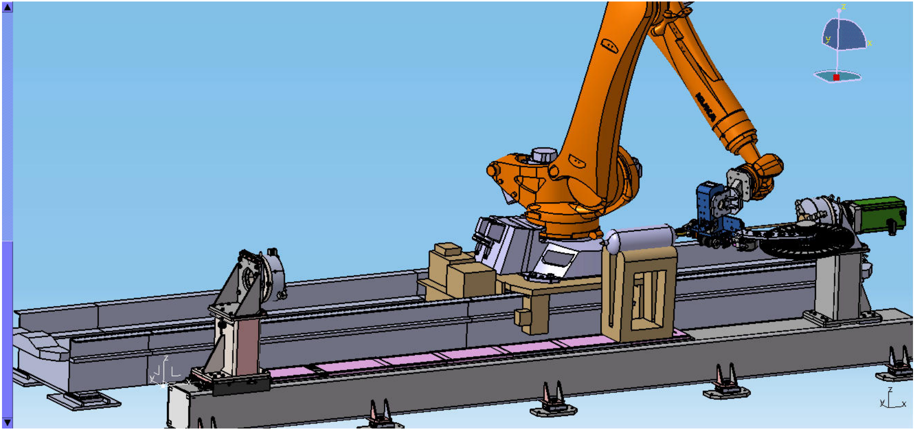

Trajectory with 200 task locations:

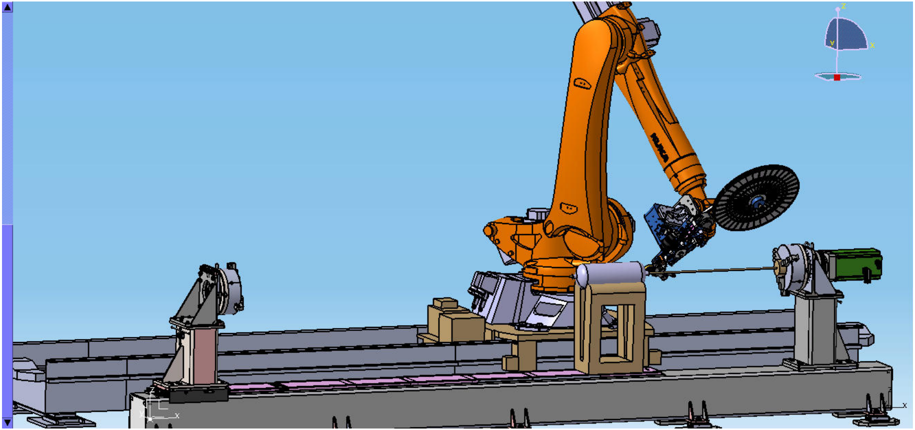

For 127 task locations, linear axis coordinate value of $-3000mm$ and with a $2deg$ discretization step for the positioner coordinate, the results obtained are as follows:

Objective Function	Travelling Time
Constant Speed	$8.4sec$
Time-Optimal	$4.7sec$

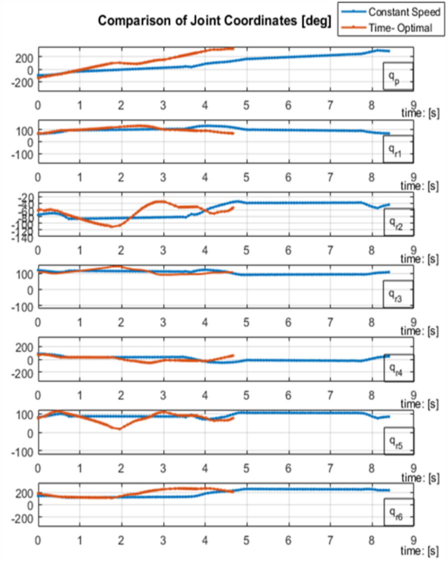

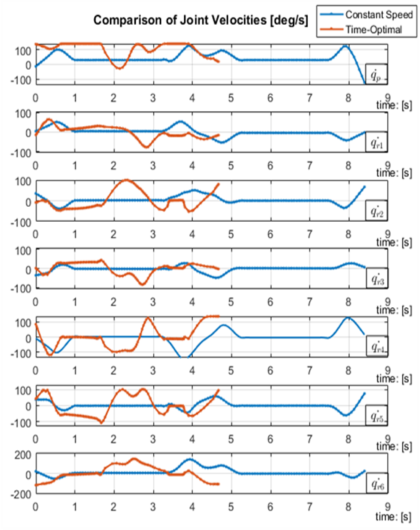
Comparison of Joint Velocities [deg/s]
Constant Speed
Time-Optimal
time: [s]

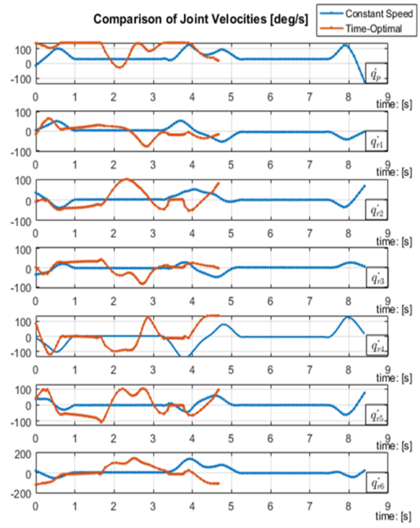
Comparison of Joint Velocities [deg/s]
Constant Speed
Time-Optimal
time: [s]

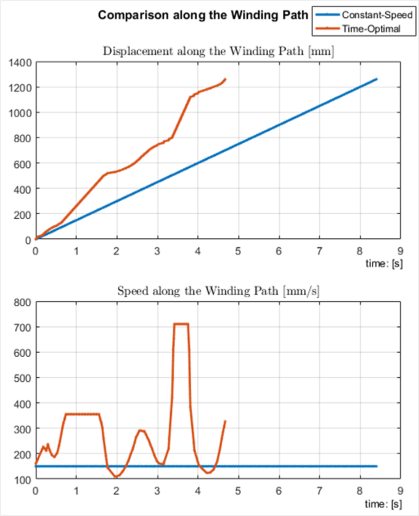
Comparison along the Winding Path
Constant-Speed
Time-Optimal
Displacement along the Winding Path [mm]
time: [s]
Speed along the Winding Path [mm/s]
time: [s]

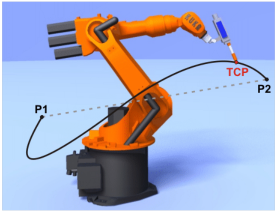

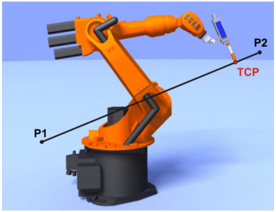

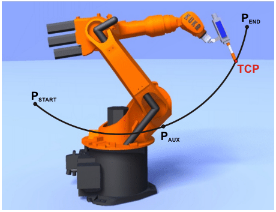

KUKA System Software 8.2, Operating and Programming Instructions for System Integrators (2011).

PTP	LIN/CIRC	SPLINE
Discrete start-stop movement	Continuous movement	Continuous movement
Joint space interpolation	Cartesian space interpolation	Both
Exact positioning	Approximate positioning	Exact positioning
Does not allow time adjustment	Does not allow time adjustment	Allows time adjustment


cetim

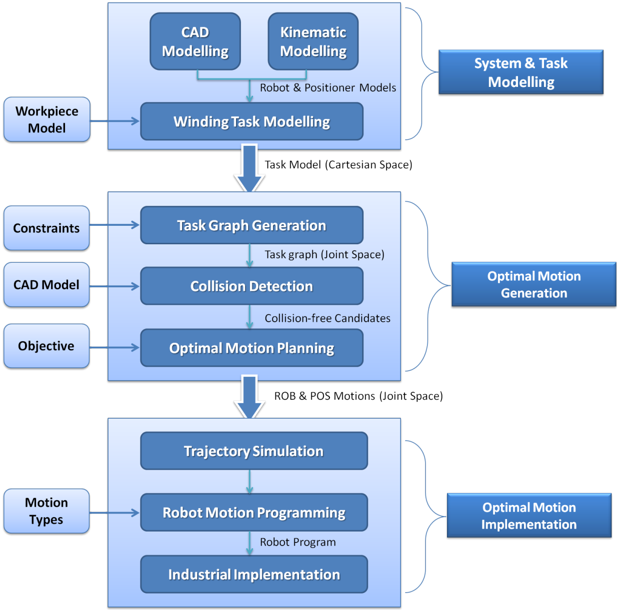
CAD Modelling
Kinematic Modelling
Robot & Positioner Models
Workpiece Model
Winding Task Modelling
System & Task Modelling
Task Model (Cartesian Space)
Constraints
Task Graph Generation
Task graph (Joint Space)
CAD Model
Collision Detection
Collision-free Candidates
Objective
Optimal Motion Planning
Optimal Motion Generation
ROB & POS Motions (Joint Space)
Trajectory Simulation
Motion Types
Robot Motion Programming
Robot Program
Industrial Implementation
Optimal Motion Implementation

- Development of CAD model to complement the computational algorithm.
- Intensive and robust collision detection.
- Time-optimal trajectories for the system.
- Simulation results show reduction of processing time by **75%**.
- The methodology will be presented and published at *The* 3^{rd} *International Conference on Mechanical Engineering (ICOME), 2017*, to be held in Surabaya, Indonesia; on October 5^{th}-6^{th}, 2017.

- Development of CAD model to complement the computational algorithm.
- Intensive and robust collision detection.
- Time-optimal trajectories for the system.
- Simulation results show reduction of processing time by **75%**.
- The methodology will be presented and published at *The* 3rd *International Conference on Mechanical Engineering (ICOME), 2017*, to be held in Surabaya, Indonesia; on October 5th-6th, 2017.

- Development of CAD model to complement the computational algorithm.
- Intensive and robust collision detection.
- Time-optimal trajectories for the system.
- Simulation results show reduction of processing time by **75%**.
- The methodology will be presented and published at *The* 3^{rd} *International Conference on Mechanical Engineering (ICOME), 2017*, to be held in Surabaya, Indonesia; on October 5^{th}-6^{th}, 2017.

- Development of CAD model to complement the computational algorithm.
- Intensive and robust collision detection.
- Time-optimal trajectories for the system.
- Simulation results show reduction of processing time by **75%**.
- The methodology will be presented and published at *The* 3^{rd} *International Conference on Mechanical Engineering (ICOME), 2017*, to be held in Surabaya, Indonesia; on October 5^{th}-6^{th}, 2017.

- Development of CAD model to complement the computational algorithm.
- Intensive and robust collision detection.
- Time-optimal trajectories for the system.
- Simulation results show reduction of processing time by **75%**.
- The methodology will be presented and published at *The* 3^{rd} *International Conference on Mechanical Engineering (ICOME), 2017*, to be held in Surabaya, Indonesia; on October 5^{th}-6^{th}, 2017.

- Testing for trajectories with different geometries and complexities.
- For workpiece liners with large lengths, use of linear axis on-line (8 DOF).
- Appropriate calibration methods to eliminate dimensional inaccuracy.
- Ways to reduce computing time, especially in collision detection.
- Optimizing the workpiece placement or the cell layout.

- Testing for trajectories with different geometries and complexities.
- For workpiece liners with large lengths, use of linear axis on-line (8 DOF).
- Appropriate calibration methods to eliminate dimensional inaccuracy.
- Ways to reduce computing time, especially in collision detection.
- Optimizing the workpiece placement or the cell layout.

- Testing for trajectories with different geometries and complexities.
- For workpiece liners with large lengths, use of linear axis on-line (8 DOF).
- Appropriate calibration methods to eliminate dimensional inaccuracy.
- Ways to reduce computing time, especially in collision detection.
- Optimizing the workpiece placement or the cell layout.

- Testing for trajectories with different geometries and complexities.
- For workpiece liners with large lengths, use of linear axis on-line (8 DOF).
- Appropriate calibration methods to eliminate dimensional inaccuracy.
- Ways to reduce computing time, especially in collision detection.
- Optimizing the workpiece placement or the cell layout.

- Testing for trajectories with different geometries and complexities.
- For workpiece liners with large lengths, use of linear axis on-line (8 DOF).
- Appropriate calibration methods to eliminate dimensional inaccuracy.
- Ways to reduce computing time, especially in collision detection.
- Optimizing the workpiece placement or the cell layout.

Thank You!!!

divya-haresh.shah@eleves.ec-nantes.fr